VERSITA

Central European Journal of **Physics**

Instability transitions and ensemble equivalence in diffusive flow

Research Article

Meesoon Ha*

Department of Physics, Korea Advanced Institute of Science and Technology, Daejeon 305-701, Korea
School of Physics, Korea Institute for Advanced Study, Seoul 130-722, Korea

Abstract: We investigate the critical behavior of one-dimensional (1D) stochastic flow with competing nonlocal and local hopping events, in context of the totally asymmetric simple exclusion process (TASEP) with a defect site in a 1D closed chain. The defect site can effectively generate various boundary conditions, controlling the total number of particles in the system. Both open and periodic-like setups exhibit dynamic instability transitions from a populated finite density phase to an empty road (ER) phase as the nonlocal hopping rate increases. In the stationary populated phase, strong clustering promoted by nonlocal skids drives such transitions and determines their scaling properties. By static and dynamic simulations, we locate such transition points, and discuss their nature and scaling properties. In the open TASEP variant, we numerically establish that the instability transition into the ER phase is second order in the regime where the entry point reservoir controls the current, while it is first order in the regime where the bulk controls the current. Since it is well known that such transitions are absent in the periodic TASEP variant, we compare our results in the open setup with those in the periodic-like setup, and discuss the issue of the ensemble equivalence. Finally, the same discussion is extended to the symmetric cases.

1. Introduction

For a long time, driven diffusive systems of particles with some local rules and some reasonable interactions have been widely studied as a prototype of nonequilibrium steady states [1]. Interestingly, systems far from equilibrium can undergo nonequilibrium phase transitions between different steady states as the control parameters of systems vary, either discontinuously or continuously, even in one dimension, which is very unlikely in equilibrium cases. So it is important to check how robust they are with respect to new dynamics once they are found. Such research is an endeavor to understand the unusual behaviors of discrete elements with the cooperative dynamics in dissipative systems, e.g., traffic or granular flow [2], the motion of stuck and flowing grains in a sand pile [3], phase separation in the steady sedimentation of a colloidal crystal [4–6], and the motion of molecular motors

*E-mail: msha@kaist.ac.kr

Springer

driven by ATP [7–9].

In this paper, we study how clustering and coarsening dynamics affect one–dimensional (1D) driven diffusive flow with a simple variant of the parking garage model [10]. The original parking garage model was proposed as the bare–bone version of dynamic Bose condensation and queuing phenomena, where traffic jams caused by so-called *bottleneck phenomena* were investigated on the defect site, namely the parking garage with infinite capacity. It is found that the model yields nonequilibrium phase transitions with macroscopic car condensation among three different types of uniform steady state according to the fraction of parked cars and steady–state current, namely Condensed (C), Maximal-Current (MC), and Normal (N) phases. In the modified version, we newly add nonlocal hopping to the totally asymmetric simple exclusion process (TASEP) [11, 12] and also consider the symmetric simple exclusion process (SSEP) [13, 14], respectively. Due to the fact that nonlocal hopping promotes clustering and coarsening and cause new instability to conventional steady–state phases, we expect dynamic phase transitions and their critical behaviors. Moreover, based on possible mappings of the SEP onto other processes, we are able to discuss similar studies with the well-known mass dynamics, the zero-range process (ZRP) [15–17] and the mass aggregation–chipping models [18–23], the well-known surface growth models, the body-centered solid-on-solid (BCSOS) model [24–27], the ballistic deposition (BD) model, and the BD variant [28, 29], and the spin exchange dynamics, namely Toom model and $\mathcal{M}^{(k)}$ model [30, 31].

In the context of traffic, nonlocal hopping may not be such a common phenomenon. However, it may occur at freeways without any speed limit, under wet or icy roads due to weather, and in some special situation of nonstop roads, e.g., before and after some big sport games or concerts, since under such circumstances either cars or drivers tend to be just behind their front car as long as they avoid any accidents. To make use of the earlier results of the original parking garage model, we here address the role of nonlocal hopping on 1D driven diffusive systems in traffic–wise point of view first, and then discuss its general aspects later.

The following two main questions are posed in this paper: **Does this new instability yield new phase transitions at its finite value?** *If so, how does clustering induced by nonlocal stick–slip events affect such transitions and scaling properties?* To answer them, this paper is organized as follows: Section 2 describes the original parking garage model and its modification with nonlocal hopping. In Sec. 3, we show schematic phase diagrams with single-site mean–field approximations and propose simple intu-

itive arguments about the nature of newly existing phase transitions. We present extensive numerical simulation results in Sec. 4, in terms of the finite–size scaling analysis and correct the MF phase diagrams. Finally, in Sec. 5, we conclude this paper with final remarks and open questions.

2. Model

Consider a one-dimensional (1D) closed road (chain) of N_s sites with a parking garage at site N_s, so that the road begins at the exit of the garage and ends at the entrance to the garage. Each site on this road, $1 \leq x \leq N_s - 1$, is either empty or occupied by at most one car, $n_x = 0, 1$, while the garage at site N_s has no occupation upper limit, $n_p \equiv n_{N_s} = 0, 1, 2, 3, ...$ It is noted that the actual upper limit of n_p is determined by the initially given total number of cars (N_c) which is conserved in the system. In the modified parking garage model, we consider two more control parameters: One is the nonlocal hopping probability as $p \in [0, 1]$ and the other is the bias of the hopping direction as $r \in [0, 1]$ as shown in Fig. 1. We use random sequential updating as in the original model.

Here is the detailed dynamic rules for the case of $r = 1$, *i.e.*, TASEP variant only (see Fig. 1 for other values of r): At each time step $t \rightarrow t + 1$, choose one site with equal probability $1/N_s$. If the chosen site, i, belongs to the road, $1 \leq i \leq (N_s - 2)$, and has a car with empty nearest-neighbor site, then the car moves either to the site $i + m$ with probability p (nonlocal hopping) or to the site $i + 1$ (local hopping) with probability $(1 - p)$ where m is its possible maximum displacement up to the site just behind its front car ($m \geq 1$ always). Near, and at the garage site, the dynamics rules are slightly modified due to the garage allowing multiple occupancy and the exit probability α, independent of the number of cars at the garage site. Note that we do not allow passing the garage and nonlocal hopping of the car that just exits from the garage site is allowed to keep the role of car reservoir and slow bond, so that the process occurs with $1 \leq m \leq N_s - i$. The modified parking garage model has three control parameters, the total car density $\rho_o = N_c/N_s$, the exit probability α at the garage site, and the speeding-up probability p on the road. For convenience, we define $\rho_p(t) = \frac{N_p(t)}{N_s}$ and $\rho_r(t) = \frac{N_r(t)}{N_s}$, where $N_p(t) = \langle n_p(t) \rangle$ and $N_r(t) = \sum_{i=1}^{N_s-1} \langle n_i(t) \rangle$ with $N_c = N_p(t) + N_r(t)$, such that $\rho_0 = \rho_p(t) + \rho_r(t)$. It is noted that the parking garage plays a role of a reservoir of the road, so the ordinary model is equivalent to the open TASEP with the injection probability α and the removal probability setting to be 1, provided that it is macroscopically occupied as long as the total car (particle) density, ρ_0, is large enough to be
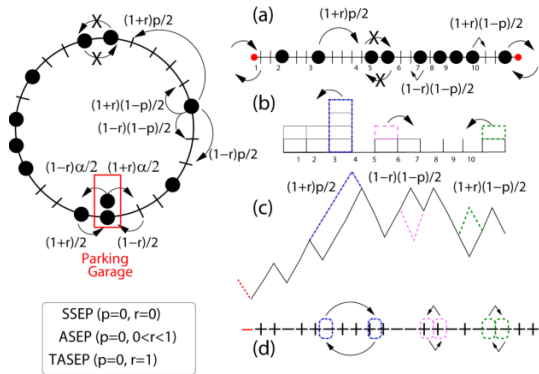
Figure 1. The modified parking garage model with nonlocal hopping and its possible mappings to other studies: (a) open SEP with nonlocal hopping, (b) open ZRP and mass aggregation-chipping model with diffusion, (c) BCSOS-type surface growth with BD interface dynamics, and (d) spin exchange dynamics. It is noted that the same color represents the same dynamic rule with the same probability, but the role of the parking garage is slightly modified for each case (see the text for the detailed mapping procedure).

compared with ρ_r. We here consider both the open setup ($\rho_r|_{t\to\infty} < \rho_0$, *i.e.*, $\rho_p \neq 0$) and the periodic–like setup ($\rho_r|_{t\to\infty} = \rho_0$, *i.e.*, $\rho_p = 0$).

As p increases, it promotes clustering and coarsening towards a phase-ordered state. The $p = 0$ case corresponds to the original parking garage model consisting of three disordered phases where cars on the road are uniformly distributed with or without macroscopic car condensation in the parking garage. In another trivial limit, $p = 1$, all conventional phases become unstable and eventually reach only one segregated state, namely the Fully-Condensed (FC, equivalently, Empty-Road, ER) phase, where the road is empty with a complete condensation in the parking garage. We observe that the system undergoes nonequilibrium phase transitions from the FC(ER) phase to the conventional C, MC, and N phases at the nontrivial instability threshold p_c.

As is well known, the exact mapping exists between the SEP and the ZRP, where the particle of the SEP represents the site of the ZRP and the number of consecutive holes in front of the chosen particle, the headways of the SEP, represents the mass of the chosen site, the occupancies of the ZRP. Such a mapping is shown in Fig. 1 (a) and (b), where we use the number indices (from 1 to 10) for the reader. Under the well-known mapping of the local hop, the skid move (nonlocal hop) in the SEP-type model corresponds to a movement of all mass on the chosen site in the ZRP-type model (namely, the diffusion process, compared to the chipping process in which the topmost mass only

moves to the target site). Due to the fact that the total number of particles in the SEP-type model corresponds to the total number of sites in the ZRP-type model, the mapping between two models is only straightforward for the SEP-type model with periodic boundary conditions, *i.e.*, translational invariance. In our model, with the broken translational invariance due to the site defect (parking garage), it no longer goes straightforwardly. In particular, the macroscopic occupancy of the parking garage $\rho_p \neq 0$ plays a role as particle reservoirs, so the total number of particles on the road fluctuates. It means that the system size of the ZRP-type model also fluctuates when our model is mapped onto it. Thus, we only consider such a mapping in the case $\rho_p = 0$ (almost the PBC-like setup) at $p = 0$. For further connections to earlier studies [24–31] we here note two more possible mappings. As shown in Fig. 1 (c), the particle in the SEP-type model is mapped to the down step and the vacancy (hole) is the up step. Similarly, as a spin configuration, Fig. 1 (d), the particle is the – spin and the hole is the + spin. The local hop represents the exchange between two consecutive opposite steps/spins, while the nonlocal hop represents the exchange between the leftmost/rightmost up step (+ spin) in the same step/spin cluster and its left/right down step (– spin). To help the readers' understanding, three possible dynamic events are illustrated with three different colors.
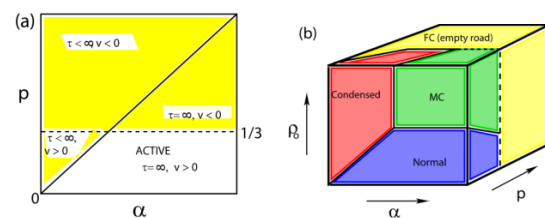

Figure 2. (a) A MF-based phase diagram of (p, α) at constant ρ_0, where the type of lines indicates first order (dashed line) and second order (solid line). (b) The extended 3D phase diagram of the parking garage model with nonlocal hopping.

3.   Mean-field approach

In order to understand qualitatively the effect of nonlocal hopping on the parking garage model, we may first consider single-site mean-field (MF) approximations. By requiring that the averaged occupation number remains unchanged ($d\langle n_i\rangle/dt = 0$) as $t \to \infty$, *i.e.*, the steady-state current should be the same everywhere:

$$\langle \tilde{\alpha}(1 - n_1) \rangle = \langle n_1(1 - n_2) \rangle, \tag{1a}$$

$$\langle n_i(1 - n_{i+1}) \rangle + p \left\langle \sum_{j=1}^{i-1} n_j \left[\prod_{k=j+1}^{i} (1 - n_k) \right] (1 - n_{i+1}) \right\rangle = \langle n_{i+1}(1 - n_{i+2}) \rangle + p \left\langle \sum_{j=1}^{i} n_j \left[\prod_{k=j+1}^{i+1} (1 - n_k) \right] (1 - n_{i+2}) \right\rangle, \tag{1b}$$

$$\langle n_{N_s-2}(1 - n_{N_s-1}) \rangle + p \left\langle \sum_{j=1}^{N_s-3} n_j \left[\prod_{k=j+1}^{N_s-2} (1 - n_k) \right] (1 - n_{N_s-1}) \right\rangle = \langle n_{N_s-1} \rangle, \tag{1c}$$

$$\langle n_{N_s-1} \rangle + p \left\langle \sum_{j=1}^{N_s-2} n_j \left[\prod_{k=j+1}^{N_s-1} (1 - n_k) \right] \right\rangle = \langle \tilde{\alpha}(1 - n_1) \rangle, \tag{1d}$$

with $\tilde{\alpha} \equiv \alpha(1 - \delta_{n_p,0})$ and $2 \leq i \leq N_s - 2$. Thus, Eq. (1c) means the steady-state "bulk" current, $J \equiv J_{i,i+1}$. It is quite difficult to solve exactly for J analytically from Eq. (1). So, taking single-site MF approximations as ignoring spatial correlations and assuming a uniform bulk density profile of $\bar{\rho} = f(p, \alpha, \rho_o)$ in the thermodynamic limit, $N_s \to \infty$, then, Eq. (1) can be rewritten as

$$J_{\mathrm{MF}}(p) = \bar{\rho} \left[(1 - p) + \frac{1}{\bar{\rho}} p \right] (1 - \bar{\rho}). \tag{2}$$

This MF current-density relation has a single maximum at $\bar{\rho}_{\max} = \frac{(1-2p)}{2(1-p)}$ as $J_{\max} = \frac{1}{4(1-p)}$ for a given value of p. Setting $\bar{\rho}_{\max} \geq 0$ (physical range), we get the stability condition of the conventional MC phase with nonzero $\bar{\rho}$ against p. The single-site MF result says that the conventional MC phase is stable as long as $p \leq p_c|_{\mathrm{MF}} = 1/2$, provided that $\rho_o \geq \bar{\rho}_{\max}$. For $p > p_c|_{\mathrm{MF}}$, $J_{\max}$ of the system is located at some negative value of $\bar{\rho}$ (unphysical), so the conventional MC phase is no longer stable since clustering and coarsening dynamics by nonlocal hopping becomes dominant. This MF threshold $p_c|_{\mathrm{MF}} = 1/2$ is quite different from what we numerically observe. However, the single-site MF result implies that the instability caused by nonlocal hopping indeed yields some new phase transitions at the finite p value.

Another evidence for the possibility of such instability transitions can be simply argued with the dynamics of the defect cluster and its stability conditions. Suppose a cluster of density ρ is located in the bulk at a distance on either side of the garage. The dynamics of this defect cluster can be characterized by the movement direction of the cluster which can be indicated by the sign of its velocity v, and its lifetime τ. Either $v < 0$ or $\tau < \infty$ means that the defect cluster would become unstable and vanish eventually, so we estimate the competition of these two stability conditions quantitatively.

Firstly, we discuss the movement of the defect cluster. It would only depend on the probability to attach one car to this cluster at the left side (front of the garage exit), $P_L \equiv \gamma p$, and the probability for the front car of this cluster to move forward (or to escape from the cluster) at the right side (toward the garage entrance), $P_R \equiv 1 - p$ (or p). Therefore, $v = 0$ means that its positive term, $(1 - p)$, is exactly canceled out by its negative term, $\left(\frac{1}{\rho} p + \gamma p \right)$, so that we get $p_c \simeq \frac{1}{3}$. Here we assume that $\gamma \simeq 1$ (one car always behind the defect) and $\rho \simeq 1$ (almost compact).

Secondly, We check the stability condition of the defect cluster and determine when its lifetime becomes finite. The change of the number of cars on the road increases and is directly related to the change of the size of the defect cluster since only one cluster is assumed in the system. The condition of $\tau < \infty$ means that the size of the defect cluster starts shrinking, i.e., the probability for one car to leave the road and to enter the garage, roughly p, becomes equal to or greater than the probability α to add one car to road from the garage, which gives $p_c = \alpha$. Whichever arises first, it becomes dominant and allows the system to attain the instability threshold, $p_c = \min \left[\alpha, \frac{1}{3} \right]$. It is claimed that that two instability thresholds exhibit the different nature of phase transitions. Figure 2 (a) shows that in the region of $\tau = \infty$ and $v > 0$ the system is only active with the conventional phases and in all other regions it reaches a phase-segregated state (kind of inactive phase with trivial fluctuations) in the steady-state limit, see Fig. 2 (b) for the extended 3D schematic phase diagram with three possible control parameters.

In the next section, our intuitive arguments are numerically confirmed and the single-site MF results are improved by the so-called cluster analysis with free and mother clusters [32], which will be compared and discussed with numerical results.

4. Numerical results and cluster analysis

To check the validity of our intuitive arguments and the MF-based phase diagrams with numerical simulation data using the finite-size scaling (FSS) technique, we perform the following Monte Carlo simulations in two different initial conditions:

1. **Stationary simulations**
   We take a finite lattice with size N_s and start with the initial condition that the particles (cars) are randomly distributed on roads with the road density $\rho_r(0) = 1/2$ and the reservoir (garage) has the remaining ones, $\rho_p(0) = \rho_0 - \rho_r(0)$. After some transient time, we measure the stationary average of various physical quantities such as the current J, the road density $\rho_r|_{t\to\infty}$, the 2nd, 3rd, 4th moments of density fluctuations, χ_m, the Binder's cumulants U_4, and the density profile $\rho(x) = \langle n(x) \rangle$, where the FSS is employed to analyze the data.

2. **Dynamic simulations**
   We start with a localized seed (actually no road particle or just one near the reservoir) in the limit $N_s \to \infty$ and observe the time-dependent properties of various quantities such as the total number of particles $N(t)$, the spreading distance $R(t)$. It is known in nonequilibrium absorbing transitions that this method is usually better than, or at least comparable with, the static one to locate the phase transition point. The critical exponent values are also obtained through dynamic scaling and hyperscaling relations. In our case, the stationary simulation data for the current provide the most accurate locations of the transition points.

Before analyzing the numerical data, we note the following analytic results.
First, we find the ER (FC) phase where the density profile is characterized by the exponential decay from the reservoir, so that the steady-state current far from the reservoir (garage) (where the exponential tail does not reach) can be written rigorously as

$$J_{ER} = p\left(1 - P(0)\right), \qquad (3)$$

where $P(0)$ is the probability that the road is completely empty, *i.e.*, $P(N_r = 0)$. This tells us that the maximal current in the ER phase, $J_{ER}|_{\max} \leq p$, which can be realized only along the ER-C and ER-MC phase boundaries where we expect $P(0) = 0$. Therefore, $J = p$ at the transition point. This condition turns out to be very useful and effective to locate the phase boundaries accurately in stationary Monte Carlo simulations. In fact, $P(0)$ may serves as another *order* parameter which becomes nonzero in the ER phase, while it vanishes in the C and the MC phases (both continuously). The critical behavior of $P(0)$ is still under investigation and will be discussed independently elsewhere[1].

Second, one can derive the upper and lower bound of the current analytically. Since the current J should increase with p, it should be constrained between $J(p = 0)$ and $J(p = 1)$, where the lower bound $J(p = 0) = \alpha(1 - \alpha)$ for $\alpha < 1/2$; $J = 1/4$ for $\alpha > 1/2$, and the upper bound $J(p = 1) = \alpha/(1 + \alpha)$. In the steady state, only two states are allowed: completely empty state $|0\rangle$ and single particle state $|1\rangle$ at site $x = 1$. From the master equation $\dot{P}(0) = pP(1) - \alpha P(0)$, we find the steady-state probabilities satisfy the relation $P(1) = (\alpha/p)P(0)$. The normalization constraint $P(0) + P(1) = 1$ gives us $P(0) = p/(p + \alpha) = 1/(1 + \alpha)$. This upper bound is exactly the same as that found previously for the current by requiring the positiveness of the vacancy-vacancy correlation, $\langle (1 - n(1))(1 - n(2)) \rangle \geq 0$. The exact bounds for the current combining with the requirement $J = p$ at the phase boundaries confine the ER-C and ER-MC transition lines in the region of $\alpha(1 - \alpha) \leq p \leq \alpha/(1 + \alpha)$ for $\alpha < 1/2$ and $1/4 \leq p \leq \alpha/(1 + \alpha)$ for $\alpha > 1/2$.

Third, we may further restrict the current value in the ER phase. The relation $P(1) = (\alpha/p)P(0)$ is true for any p (even though $P(1)$ now represents the probability that the system contains one particle anywhere on the road), but the normalization constraint yields an inequality $P(0) \leq p/(p + \alpha)$ for any p. This leads to the lower bound of $J_{ER} \geq \alpha p/(p + \alpha)$, which further restricts J_{ER} for $p > 1/3$. However, unfortunately, we cannot find any use for this information presently within our results.

Finally, one may simply try improved MF approximations, which consider intrinsic spatial inhomogeneities systematically. We indeed test such approximations by considering inhomogeneity in only a few sites near the reservoir, because the inhomogeneity is expected to be important only nearby the reservoir, and find that they still fail to explain the phase diagram obtained by our numerical simulations. Ultimately, that is why we develop the cluster analysis.

For more precise analysis near the transition lines and the scaling properties of the new continuous C-FC(or FC-C) transition, we use the following techniques:
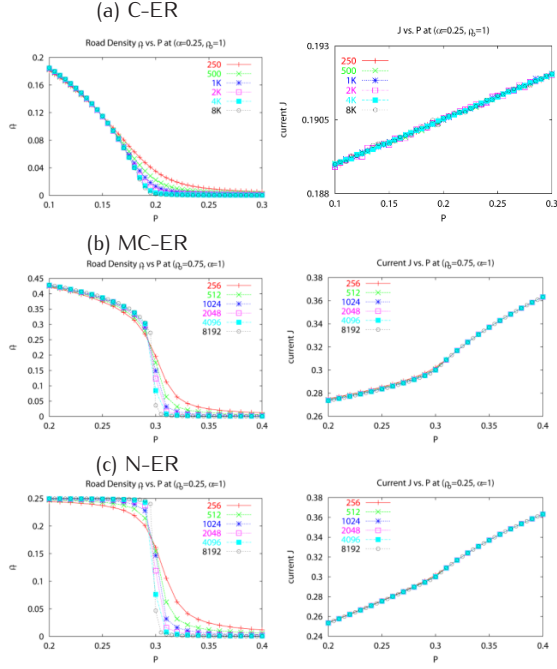
---

[1] *M. Ha, H. Park (unpublished)*

(a) C–ER

(b) MC–ER

(c) N–ER

Figure 3. Numerical data for the road density ρ_r and the averaged current J for various system sizes: (a) the C-FC transition, (b) the MC-FC transition, and (c) the N-FC transition. Here FC represents ER in [32].

In static simulations, one can estimate the values of critical exponents by exploiting conventional FSS relations as

$$
\begin{aligned}
\rho_r &= L^{-\beta/\nu} f(\Delta N_s^{1/\nu}), \\
\chi_2 &= L^{\gamma/\nu} g(\Delta N_s^{1/\nu}), \\
U_4 &= h(\Delta N_s^{1/\nu}),
\end{aligned}
\tag{4}
$$

where $\Delta = (p_c - p)$ or $(\alpha - \alpha_c)$ is a measure of the distance from the transition and ν is the correlation length exponent. The functions f, g, and h are scaling functions. Elementary scaling ansatz yields the hyperscaling relation such as $(2\beta + \gamma)/\nu = d = 1$. Here we take the system size $N_s = 256$ (250 in some case) $\times 2^n$ with $n = 1, 2 \cdots, 6$ and discard data up to $t \simeq N_s^2$ for equilibration and collect data up to $t = 10^8 \sim 10^9$ at every Monte Carlo step (one sweep over the lattice). Next, our data are averaged over $10 \sim 200$ independent Monte Carlo runs.

In dynamic simulations, we start with no particle and observe the evolution of the number of particles on the road $N(t)$ and the position of the rightmost particle $R(t)$. We expect that these quantities scale at criticality as

$$
\begin{aligned}
N(t) &= t^\theta, \\
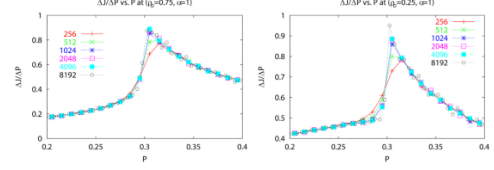R(t) &= t^{1/z},
\end{aligned}
\tag{5}
$$

Figure 4. $\Delta J/\Delta p$ versus p for various system sizes: MC-FC transition (left) and N-FC transition (right), which tell us that the transitions are first order.
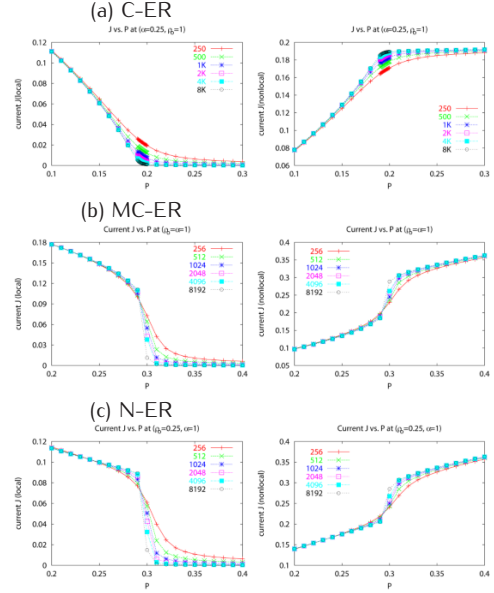

(a) C–ER

(b) MC–ER

(c) N–ER

Figure 5. Decomposition of J to local and nonlocal portions for various system sizes: (a) the C-FC transition, (b) the MC-FC transition, and (c) the N-FC transition.

where θ is the growth exponent and z is the dynamic exponent. One can easily derive the dynamic hyperscaling relation as $\theta z + \beta/\nu = d = 1$. Our data are averaged over $10^4 \sim 10^5$ independent runs up to $t = 10^5$ for $N_s = 10^6$. Among our numerical results summarized in Table 1, Table 2, and Table 3, we show only two specific cases in detail: $\left(\rho_0 > \frac{1}{2}, \alpha, p\right)$ as the open setup and $(\rho_0 = 1/4, \alpha = 1, p)$ as the periodic–like setup, respectively. It is noted that other cases are similar to those two.

We consider two major physical quantities as possible indicators of dynamic instability transitions: the road density, $\rho_r (\equiv \rho_r|_{t\to\infty})$, and the averaged current, J, in the steady–state limit up to $N_s = 8192$ (8000 in some cases).

The FSS effect of numerical data is shown in Fig. 3. At the C-FC transition ($\alpha < \alpha^*$, $\rho_0 = 1$), ρ_r plays a crucial role as the indicator of a new continuous phase transition, see Fig. 3 (a), where J has no singular point, while both ρ_r

Table 1. Critical values and exponents (C-ER).

α	0.1	0.2	0.3	0.4
p_c	0.09008(8)	0.16125(5)	0.21553(8)	0.25521(4)
$(U_4)_c$	0.01(5)	0.08(3)	0.07(2)	0.15(4)
$1/\nu$	0.50(5)	0.50(2)	0.50(3)	0.50(2)
β/ν	0.49(1)	0.48(2)	0.47(3)	0.45(5)
γ/ν	0	$(\log(N_s)$	also	works.)
p_c	0.0900(2)	0.16120(5)	0.2156(1)	0.25515(5)
θ	0.52(2)	0.508(8)	0.505(5)	0.510(5)
$1/z$	0.98(2)	0.97(3)	0.95(5)	0.90(5)
R	$\sim t/(\log(t))^{a<0.5}$	0.5(1)	0.6(2)	1.2(2)

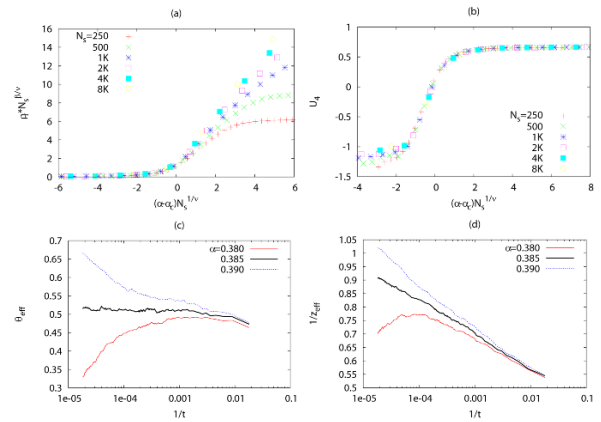**Table 2.** First-order transition values and exponents (MC-ER).

α	0.7	0.75	0.85	1.0
p_c	0.2990(5)	0.2990(4)	0.2990(2)	0.2990(3)
$(\rho_r)_c$	0.17(1)	0.16(1)	0.16(1)	0.16(1)
$(U_4)_c$	0.46(8)	0.47(2)	0.47(3)	0.45(7)
$1/\nu$	0.9(1)	0.8(2)	0.9(1)	0.85(15)
p_c		0.2990(2)		0.2989(1)
θ		0.500(5)		0.485(5)
$1/z$		0.55(1)		0.545(5)
R		0.6(1)		0.5(1)

Table 3. At constant p, continuous and Discontinuous transition values and exponents (ER-C and ER-C/MC).

p	0.25	0.27	0.299
α_c	0.385(5)	0.450(3)	0.64(1)
$U_4(p_c)$	0.197(9)	0.20(2)	0.33(1)
β/ν	0.51(1)	0.51(1)	0.10(1)
γ/ν	0.21(1)	0.23(2)	0.83(2)
$(\chi_2)_m \sim$	$\log(N_s)$	$\log(N_s)$	$N_s/\log(N_s)^{1.4(1)}$
$1/\nu$ (U_4 data)	0.50(4)	0.50(4)	0.50(4)
$1/\nu$ (ρ_r data)	0.50(5)	0.50(5)	0.50(5)
α_c	0.385(3)		0.630(4)
θ	0.50(3)		0.475(9)
$1/z$	0.94(6)		0.536(5)
$R \sim$	$t/(\log(t))^{0.6(2)}$		$t^{1/2}(\log(t))^{0.4(1)}$

Figure 6. At $p = 0.25$ and $\rho_0 = 1$, data collapse plots of (a) ρ_r and (b) U_4 with $\alpha_c = 0.385$, $\beta/\nu = 0.51$, and $1/\nu = 0.50$, and effective exponent plots in dynamic simulations: (c) θ and (d) $1/z$. Based on the effective exponent plots, we can determines the value of α_c as well as the values of z and θ at the same time, which are shown in Table 3.

and J play a role of good indicators for new discontinuous phase transitions as $\rho_r \to 0$ and J becomes singular at the MC–FC transition ($\alpha > \alpha^*$, $\rho_0 > \rho_0^*$) and the N–FC transition ($\alpha = 1$, $\rho_0 < \rho_0^*$) as shown in Fig. 3 (b) and (c), respectively. Up to the C–MC transition point α^*, the value of p_c does depend on α (the larger α, the larger p_c), while for $\alpha > \alpha^*$, the system undergoes another instability threshold, whose value is the same as that at $\alpha = 1$ ($p_c \simeq 0.3$). It is observed that two second–order transition (C–ER and C–MC) lines merge into a first–order transition line at the same end point (see Fig. 4). The first–order transition line, MC–ER, seems to be almost flat. The total current J starts to increase linearly with α and slowly saturates to a p-dependent value. The ER-C transition point identified by requiring $J = p$ is in excellent agreement with that obtained by other numerical techniques. For better understanding the critical behavior, we decompose J to the local and nonlocal portions, which are shown in Fig. 5.

Combining all results, we conjecture that the C–ER transition is characterized by the MF exponents such as $\beta = 1$, $\gamma = 0$ (log), $\nu = 2$, $\theta = 1/2$ and $z = 1$. Similarly, the MC–ER transition occurs at the same p values independent of

$\alpha \geq 0.7$. Across the transition, there is a discontinuous jump in ρ_r with the exponents as $\beta = 0$ (jump), $\gamma = 1$ (with $1/\log(N_s)$ corrections), $\nu = 1$, $\theta = 1/2$ and $z = 2$ (some log corrections). Our complete lists for numerical results for the C–ER transition and the MC–ER transition are tabularized in Table 1 and Table 2, respectively. When we fix p and vary α in the open setup ($\rho_p \neq 0$), we can observe the ER-C and C–MC transitions, or the ER-C/MC transition, which depends on the value of p. As shown in Table 3 and Fig. 7, we encounter two transitions, ER(FC)–C and C–MC, for $p < 0.3$ as α increases. The latter (C–MC) transition has also been studied in the original parking garage model [10], so we here focus on the former (ER-C) transition only. The critical behavior
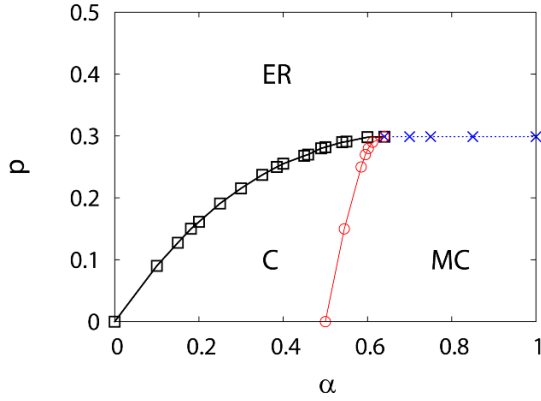
Figure 7. The 2D $\alpha - p$ phase diagram from our numerics in the open setup.

of the order parameter ρ_r at and near the ER-C transition obeys the same FSS relation with the same exponent set, so

$$\rho_r(\Delta, N_s^{-1}) = N_s^{-\beta/\nu}\Psi(N_s^{1/\nu}\Delta), \qquad (6)$$

where $\Delta = \alpha - \alpha_c$. Based on inflection criteria for successive slopes of ρ_r, we estimate the FSS exponent β/ν and α_c at the same time, which are consistent with those in Table 1. Our numerical data collapse very well (see Fig. 6). Note that the instability threshold α_c seems to be independent of the total car density ρ_0. As long as $p < 0.3$, the system exhibits a new continuous phase transition besides two conventional phase transitions in the (ρ_0, α) phase diagram at fixed p values. We numerically investigate the locations of the C-N and MC-N transition lines at nonzero p and find that the location of the conventional transition lines depends on p. Since it turns out that their universality class remains the same as before in the original parking garage model [10], we will not present them in detail.

Our numerical data correct the MF phase diagram as Fig. 7, which can be also argued by the so-called cluster analysis. We adopt the clustering point of view for the steady-state configurations in the C-type and MC-type phases once $p \neq 0$, where two kinds of clusters exist. One is the free cluster that is located in the bulk far from the reservoir (garage), and the other is the mother cluster that is attached to the reservoir. Since the detailed cluster analysis can be found in Sec. III and Sec. IV of Ref. [32], we briefly recall its basic concept and main results. By definition, the steady state has the same current everywhere, so the current of the free cluster should be the same as that of the mother cluster. Let us consider that each cluster consists of three parts, the front part, the rear, and the bulk (the center of mass for a given cluster), write down the corresponding currents in terms

of MF-type approximations and find the conditions when they have the same values as the maximal current value. As a result, we can find the following results: the C-ER (or ER-C) transition occurs due to the instability of the mother cluster by the small value of α, while MC-ER transition eventuates due to the instability of the free clusters. Moreover, we have argued the nature of phase transitions and scaling properties as well as the locations of p_c. The similar cluster analysis has been applied to the symmetric case [33], where the ensemble equivalence issue has also been discussed.

5. Conclusions

We have addressed how nonlocal dynamics affect one-dimensional (1D) nonequilibrium driven diffusive flow, in context of the modified parking garage model by the totally asymmetric simple exclusion process (TASEP) with nonlocal hopping. By which, large-scale clustering and coarsening in conserved systems are promoted. It would be an especially interesting possibility for the behavior of two coupled systems: one of which evolves autonomously but influences the dynamics of the other. Unlike the condensed (C) to fully condensed (FC) transition, the maximal current (MC) or normal (N) to FC (or Empty Road, ER) transition is very sharp. The reasonable answer for the origin of this discontinuous transition is the long-ranged character of the interaction, which is responsible for phase separation. This phenomenon is reminiscent of colloidal sedimentation in suspending flows, resulting from the balance between gravity and viscosity. In both cases, macroscopic phase separation is observed, which is robust as long as the instability exists. This kind of phase separation might be understood in terms of barriers to remixing which grow with system size and result in a somewhat slow approach to the steady state. In addition, we need to figure out how the result of the periodic-like setup is different from that of the periodic setup in order to discuss the ensemble equivalence issue for the asymmetric case, compared to earlier studies that do not exhibit any phase transitions (neither clustering nor condensation) in the thermodynamic limit[1] [20–23].

In the experimental point of view, it would be interesting to discuss a dramatic clumping transition as all cars form a condensate in the garage, namely the N-FC transition. This implies that 1D naturally driven diffusive flow will do so as well. Such transitions can be observed in many real physical systems, such as the sedimentation of charged/uncharged colloidal crystals [5, 6], where the main issue is how to reduce the repulsion between polyballs. Therefore, one may mimic realistic interactions be-

tween balls besides on-site repulsion. However, it first needs to manifest the most general case (analytically more tractable). One can also find the relationship of our work to earlier work on related models where nonlocal hopping can be mapped to local diffusion in mass dynamics as, for instance, in Ref. [18, 19], which contained a mass-conserving coalescence process with $p = 1$; in Ref. [20–22], which focused on steady-state mass distribution in the conserved-mass model with aggregation (nonlocal hopping rate: 1) and fragmentation (local hopping rate: w) without spatial bias; in Ref. [23], which discussed the biased conserved-mass model. The detailed relationship of our results to earlier results is in preparation[1].

Acknowledgements

References

[1] B. Schmittmann, R. K. P. Zia, In: C. Domb, J. Lebowitz (Eds.), Phase Transitions and Critical Phenomena, Vol. 17. (Academic, London, 1995)

[2] M. Schrenckenberg, D. E. Wolf (Eds.), Traffic and Granular Flow'97 (Springer-Verlag, Singapore, 1998)

[3] P. Biswas, A. Majumdar, A. Mehta, J. K. Bhattacharjee, Phys. Rev. E 58, 1266 (1998)

[4] R. Lahir, S. Ramaswamy, Phys. Rev. Lett. 79, 1150 (1997)

[5] M. A. Rutgers, J.-Z. Xue, E. Herbolzheimer, W. B. Russel, P.M. Chaikin, Phys. Rev. E 51, 4674 (1995)

[6] S. E. Paulin, B. J. Ackerson, Phys. Rev. Lett 64, 2663 (1990)

[7] M. E. Fisher, A.B. Kolomeisky, Physica A, 274, 241 (1999)

[8] T. Harms, R. Lipowsky, Phys. Rev. Lett. 79, 2895 (1997)

[9] F. Jülicher, J. Prost, Phys. Rev. Lett. 78, 4510 (1997)

[10] M. Ha, M. den Nijs, Phys. Rev. E 66, 036118 (2002)

[11] B. Derrida, M. R. Evans, V. Hakim, V. Pasquier, J. Phys. A 26, 1493 (1993)

[12] B. Derrida, E. Domany, D. Mukamel, J. Stat. Phys. 69, 667 (1992)

[13] B. Derrida, B. Doucot, P.-E. Rohche, J. Stat. Phys. 115,717 (2004)

[14] B. Derrida, J. L. Lebowitz, E. R. Speer, J. Stat. Phys. 107, 599 (2002)

[15] F. Spitzer, Adv. Math. 5, 246 (1970)

[16] O. J. O'Loan, M. R. Evans, M. E. Cates, Phys. Rev. E 58, 1404 (1998)

[17] M. R. Evans, Braz. J. Phys. 30, 43 (2000)

[18] K. Jain, M. Barma, Phys. Rev. E 64, 016107 (2001)

[19] M. Ha, H. Park, M. den Nijs, J. Phys. A 32, L495 (1999)

[20] R. Rajesh, S. N. Majumdar, Phys. Rev. E 63, 036114 (2001)

[21] S. N. Majumdar, S. Krishnamurthy, M. Barma, J. Stat. Phys. 99, 1 (2000)

[22] S. N. Majumdar, S. Krishnamurthy, M. Barma, Phys. Rev. Lett. 81, 3691 (1998)

[23] R. Rajesh, S. Krishnamurthy, Phys. Rev. E 66, 046132 (2002)

[24] M. Plischke, Z. Rácz, D. Liu, Phys. Rev. B 35, 3485 (1987)

[25] D. Dhar, Phase Transitions 9, 51 (1987)

[26] L.-H. Gwa, H. Spohn, Phys. Rev. Lett. 68, 725 (1992)

[27] L.-H. Gwa, H. Spohn, Phys. Rev. A 46, 844 (1992)

[28] P. Meakin, P. Ramanlal, L. M. Sander, R. C. Ball, Phys. Rev. A 34, 5091 (1986)

[29] H. Park, M. Ha, I.-M. Kim, Phys. Rev. E 51, 1047 (1995)

[30] B. Derrida, J. L. Lebowitz, E. R. Speer, H. Spohn, Phys. Rev. Lett. 67, 165 (1991)

[31] B. Derrida, J. L. Lebowitz, E. R. Speer, H. Spohn, J. Phys. A 24, 4805 (1991)

[32] M. Ha, H. Park, M. den Nijs, Phys. Rev. E 75, 061131 (2007)

[33] A. Nagar, M. Ha, H. Park, Phys. Rev. E 77, 061118 (2008)